7th International Building Physics Conference

IBPC2018

Proceedings

SYRACUSE, NY, USA

September 23 - 26, 2018

Healthy, Intelligent and Resilient
Buildings and Urban Environments

ibpc2018.org | #ibpc2018

Computer Tomography as a data acquisition tool for quantifying and modeling in-pore gypsum crystallization in building materials

Steven Claes[1,*], Jelena Todorovic[1] and Hans Janssen[1]

[1] KU Leuven, Department of Civil Engineering, Building Physics Section, Kasteelpark Arenberg 40, 3001 Heverlee, Belgium

[*]*Corresponding email: Steven.claes@kuleuven.be*

ABSTRACT

In the last few decades a new type of persistent efflorescence has started appearing on ceramic brick facades in the UK, the Netherlands and in Belgium. Since the problem undermines the aesthetic appearance of masonry buildings, it results in a growing number of complaints from building owners.
In the laboratory, gypsum efflorescence is typically studied via wicking tests. However, these often yield gypsum subflorescence instead, leading to significant pore clogging just below the evaporation surface. To gain further insight in that subflorescence and pore clogging, a correct quantification of the amount and the distribution of the gypsum crystalised in the pore space is necessary. Micro-CT achieves this by allowing visual inspection as well as quantitative data gathering. Because of the non-destructiveness of micro-CT, samples can be scanned before and after subflorescence/pore clogging has occurred. The suggested methodology includes visualization and characterization of the pore space. Observing the changes in pore structure, with the assumption that these are induced only by the presence of the salt crystals, it is possible to accurately quantify the volume of gypsum present, as well as the location of the affected pores in 3D. Due to the partial volume effect, the CT dataset can be used to detect objects smaller than the voxel size because the density difference between gypsum and air is large enough.
The obtained results confirm the presence of a thin gypsum layer just below the evaporation surface of the sample. Other techniques such as the wicking test and MIP also confirm the observations regarding pore size change and gypsum content.

KEYWORDS
Salt crystallization, Pore clogging, Brick sample, Micro-CT, Pore network properties

INTRODUCTION

The development of gypsum efflorescence on newly erected ceramic brick facades is a rising problem in the UK, the Netherlands and Belgium (Chwast et al, 2015). Unlike the common efflorescence, composed of soluble salts which are easily washed away by natural weathering, the new efflorescence consists of slightly soluble gypsum, which makes it persistent and hard to remove. Once formed on the masonry surface, they stay and permanently spoil the facade's appearance.
Even though salt crystallization in porous materials has already been the subject of study for many decades, there is still a lack of knowledge and understanding in relation to the involved pore clogging and its impact on the moisture transfer properties of porous materials. In order to study this phenomenon in laboratory conditions, wicking experiments are often performed.

Such experiments usually reveal gypsum's tendency to crystallize under the surface, inducing significant pore clogging and resultantly a strong drop in the wicking rate.

In this paper, the resultant changes in the brick's pore structure, with the assumption that these are induced only by the presence of the salt crystals, will be quantified based on CT datasets. It will be shown that such CT analysis makes it possible to accurately quantify the volume of salts present as well as the location of the affected pores in 3D.

METHODS

Wicking test

The effect of gypsum pore clogging is generated with a wicking test. It is composed of a brick sample fed with a gypsum solution from the bottom side, while evaporation is permitted only from the top side. The gypsum solution for the wicking test is prepared by dissolving 2.2 g of calcium sulphate dihydrate (Fisher Chemicals, 99% pure) in 1l of distilled water (conductivity of pure water 1.2µS/cm). The prepared solution is 85% saturated, and its concentration can be calculated as 2200 g/m^3. The experimental set-up is composed of a glass container with at the bottom a layer of gypsum solution. The container is closed with a plastic lid, to which a brick sample is mounted. In this way, a constant contact between the solution and the brick sample is maintained throughout the experiment. The experiment is conducted in a climate chamber, under constant environmental conditions, at 21^{o}C temperature and 40% relative humidity, for a duration of 14 days.

CT characterization

Computed tomography (CT) is a non-destructive visualization technique, generating images of slices of a sample based on the attenuation of X-rays. Hence, it enables the 3D visualization of the internal structures of the object. As CT is a fast and non-destructive technique, it has become a reliable method to analyze the heterogeneity of interior components as well as the porosity network of the studied sample. A more detailed explanation of the principles of CT can be found in Claes et al. (2018). Also Aikens (1991), Kak and Slaney (1988) and Herman (2009) provide more general information about the technique.

In order to determine the effect of the salt precipitation, the same sample is scanned by micro-CT before and after the above described wicking experiment. Both scans are performed using the same scan parameters (80 kV and 160 µA) and both have a resolution of 3.5 µm. The quantitative data are generated through the attenuation of X-rays, which are sensitive to sample density and atomic number, and are stored in voxels as relative gray scale values. Since in theory the only difference between both scans is the presence of salt, which will cause a higher attenuation of the x-rays compared to the air present in the pores of the original sample, resulting in higher greyscale values of the voxels. Thus, a subtraction of both datasets should result in the quantification of the precipitated salt. Hence, it becomes very important to subtract the correct corresponding voxels of both datasets, in order not to introduce artificial artefacts in the results. This is achieved by a registration process involving the determination of a geometrical transformation that aligns points in one view of an object with corresponding points in another view of that same object. The inputs of the registration algorithm are the two views to be aligned; the output is a geometrical transformation, which is a mere mathematical mapping from points in one view to points in the second. In order to retain cubic voxels, the values of the voxels of the transformed view will be linearly interpolated.

RESULTS & DISCUSSION

Effect on the pore network

A visual inspection of the micro-CT slices taken at the same depths from the top evaporation surface show that, in the top of the sample, gypsum is present at the edges of large pores and clogs smaller pore throats (Figure 1 A-B). Comparison of slices taken towards the bottom of the sample indicate that no visual gypsum is present (Figure 1 C-D).

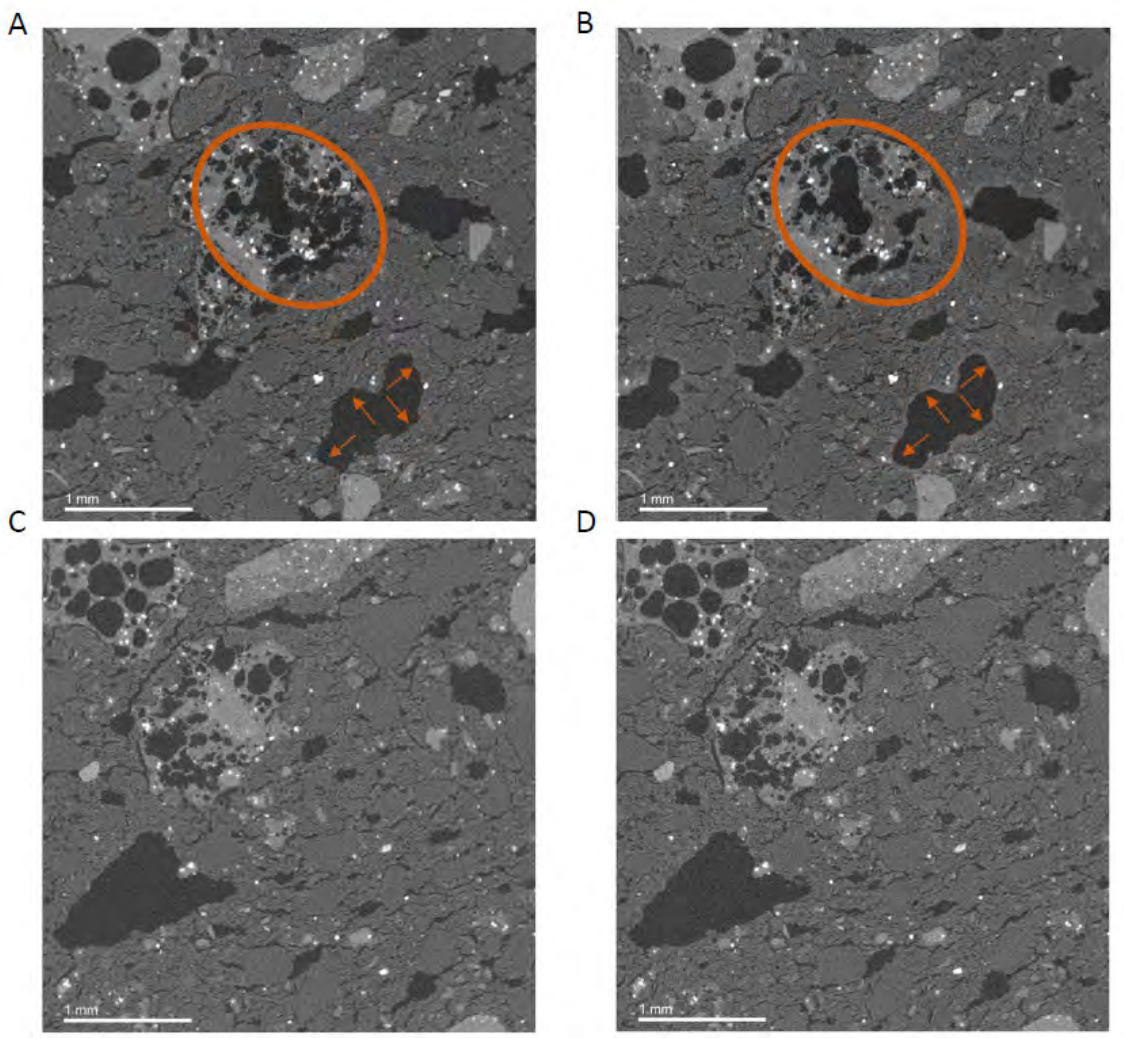

Figure 1. Micro-CT slices of the brick sample parallel to the evaporation surface. a) Original state at 130 µm bellow the evaporation surface, b) State with salt present at 130 µm bellow the evaporation surface; orange markers illustrate the differences, c) Original state at 1.5 mm from the evaporation surface, d) State with salt at 1.5 mm from the surface, no differences are visible between c and d.

These images are used to deduct the pore network in these volumes by applying a hysteresis segmentation (Claes et al., 2018). Subsequently these pore networks are split into pore bodies and pore throats using the workflow of Blunt et al. (2013).

Based on a visual inspection of the slices, the salt precipitation occurs in the top layer of the studied sample. Hence, two corresponding volumes of 500 x 500 x 120 voxels (1.75 x 1.75 x 0.42 mm³) are selected in this layer.
In general the CT-detectable open porosity is decreased by 1.2 %, from 15.6 % porosity in the original sample to 14.4 % in the affected sample. Moreover, the salt subflorescence has a clear effect on the pore size as well as on the overall distribution of pore bodies and throats in the studied volumes. As expected from the visual observations in Figure 1, the number of pore bodies and throats increases in the volume affected by salt precipitation. The average pore radii become 5 % smaller when affected by the salt. This can be explained by the rims of salt formed at the edges of the pores. Figure 2 represents the calculated pore size distributions of the reference and affected volume. The number of pores in the bin with the smallest pore radii also increases from 2460 pores to 3283. Additionally a clear shift towards smaller coordination numbers can be noticed in the sample where salt is present, even tough is has a larger number of throats in the same sample volume (8324 compared to 6777). This results in a halving of the simulated permeability but these simulations only take into account the visible porosity in the CT scan.

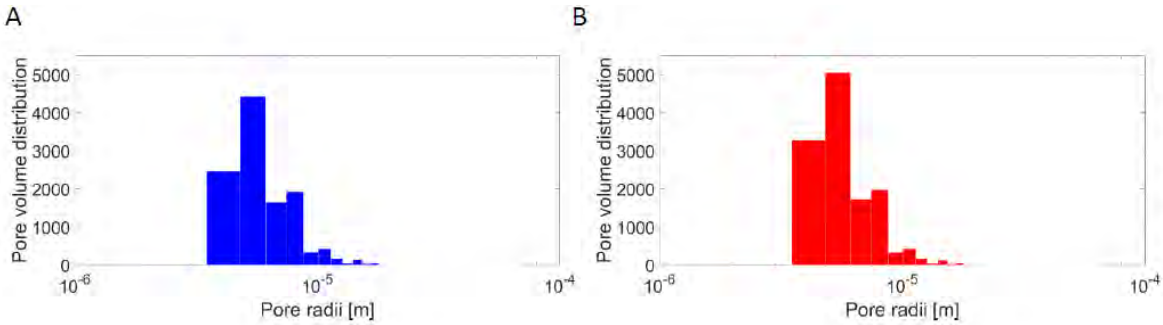

Figure 2. Pore volume distribution. a) Reference sample, b) Affected sample.

Validation
The results of the visual comparison of the slices agree with observations made in lab results and confirm the creation of a salt subflorescence layer just below the top evaporation surface. Admittedly, the influence of the scan resolution remains apparent, as only half of the open porosity can be CT-detected (15.6 % vs 31.8 % which is the actual open porosity of the brick samples). The obtained pore size distributions are further matched to distributions acquired by mercury intrusion porosimetry (MIP). Todorovic and Janssen (2018) noted that that the curves of samples containing gypsum shifted in two general directions: firstly a downward shift corresponding to a decrease in open porosity, and secondly a shift to the left, towards smaller pore radii. The same observations can be partially made based on Figure 2. It is important to notice that due to the scanning resolution of 3.5 m the spectrum of CT-detectable pore radii is limited. Hence, most of the clogged open porosity was not visible in the reference scan, since these pores fall below the resolution. The beginning of the shift to the left is visible but the main shift occurs for pores with radii of 10^{-6} m which are not captured in the micro-CT scan.

Quantification and spatial distribution of the salt
The validation of the results obtained in the prior section indicate that they are greatly affected by the limited scan resolution, as only half of the expected open pores are visible in the scan. Another approach is therefore necessary to accurately quantify the distribution of precipitated gypsum. Micro-CT datasets have the added advantage that objects smaller than the voxel size can still be detected if the density difference between the competing components is large

enough. For the studied problem this is the case because ρ_{gypsum} (2300 kg/m^3) > ρ_{air} (1.25 kg/m^3). This is due to what is generally called the partial volume effect (Figure 3 A). Because the borders of the scanned sample or a component in the sample may not coincide with the borders of the pixels of the detector, the partial volume effect occurs: features smaller than the resolution will also contribute to the attenuation coefficient of the voxel in a linear way.

Hence, in order to quantify all gypsum present in one slice, slices corresponding to the same depth are subtracted from each other. In Figure 3 B-C the histograms of these subtractions are depicted. The histogram of a slice where no salt is visible corresponds to a symmetrical bell curve centered approximately around zero. Hence this curve is interpreted as a representation of the noise present in the subtracted images. For the slices nearer to the top of the sample, the histograms become asymmetrical, and show an increase in positive difference values around 1200. These curves will therefore be modeled as a sum of two normal distributions. Parameter p represents the contribution of the noise component to the overall model, while a factor (1-p) is assumed to define the gypsum. The distributions are fitted using a maximum likelihood method. Table 1 summarizes the modeled parameters.

Table 1. Overview of typical values of the fitted parameters.

slice depth	p	μ1	σ1	μ2	σ2
0,2 mm	0.85	-112	568	903	1137
1,2 mm	0.98	5.6	620	25.5	1087

Based on these models the parameter (1-p) represents the relative amount of voxels for which the composition has changed between the two scans. Hence, they can be used to characterize the volume percentage of salt in each slice. The profile is shown in Figure 3 D and clearly indicates the presence of a gypsum crust at the top of the sample. The top 49 μm are not processed as these are too much affected by the surface roughness of the brick sample. The sudden drops in the profile can be explained by spurious additional noise in some slices.

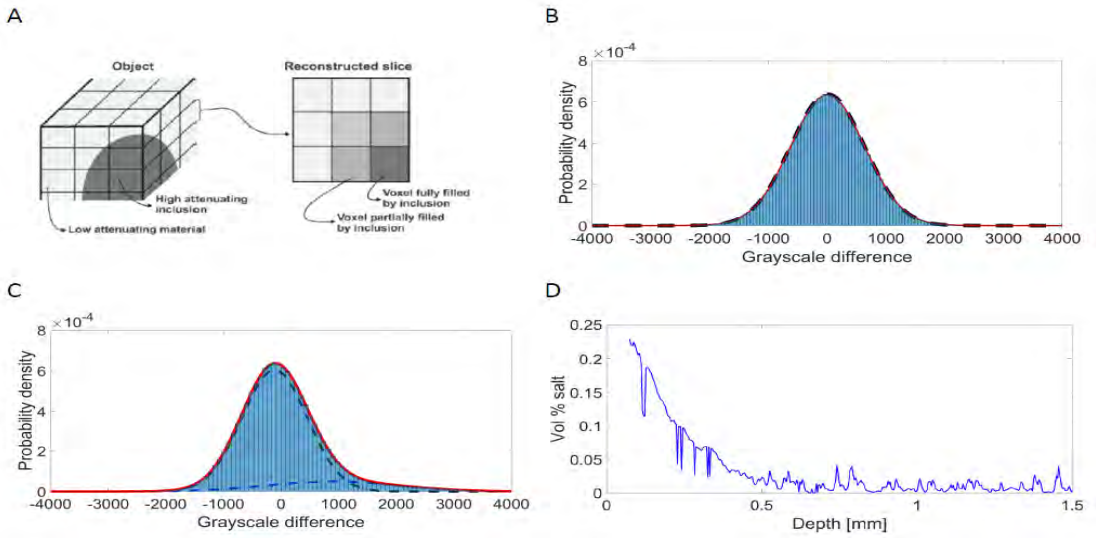

Figure 3. Localisation and quantification of the salt layer. a) Schematic overview of the linear partial volume effect (modified from Pullan et al., 1981), b) Histogram of the difference between two slices near the bottom of the sample (black dotted line represents the noise component, red line represents the overall model), c) Histogram of the difference between two slices near the top of the sample (black dotted line represents the noise component, blue

dotted line represents the salt component, red line represents the overall model), d) Volume percentage salt in function of sample depth.

Validation

In order to validate the results of the calculated presence of gypsum in the section above, these results are compared to the lab measurements. On average 0.046 g of gypsum precipitated in the 28.7 mm diameter ceramic brick plugs. This corresponds to a total amount of gypsum of 71 g/m^2. By calculating the surface below the curve in Figure 3 D up to 450 µm below the top surface, a total amount of 91 g/m^2 is obtained from our CT measurements. Both measurement methods are thus in agreement with each other.

CONCLUSIONS

In this paper the location and concentration of the gypsum subflorescence layer in bricks is successfully determined based on 3.5 µm resolution micro-CT scans. The evaporated gypsum is concentrated in the top 450 µm layer of the sample. Based on the pore network analysis general observations about the change in pore geometry can be made. However, comparison with MIP measurements indicate the strong importance of the contribution of pores below the scanning resolution. The partial volume effect can overcome some of these limitations, but additional visualization techniques with smaller resolutions will need to be used in the future in order to perform accurate fluid flow simulations.

ACKNOWLEDGEMENT

This project has received partial funding from the FWO Odysseus grant 'Moisture transfer in building materials: analysis at the pore-scale level'. Their support is kindly acknowledged.

REFERENCES

AIKENS, R. S. 1991. *Charge-Coupled Devices for Quantitative Electronic Imaging. International Amateur-Professional Photoelectric Photometry Communications*, 44**,** 1.

Blunt, M. J., Bijeljic, B., Dong, H., Gharbi, O., Iglauer, S., Mostaghimi, P., Pentland, C. 2013. *Pore-scale imaging and modelling*. Advances in Water Resources, 51, 197-216.

Claes, S., Van De Walle, W., Islahuddin, I. Janssen, H. 2018. *The application of Computed Tomography for characterising the pore structure of building materials*, IBPC 2018 (submitted).

Chwast, J., Todorovic´, J., Janssen, H., Elsen, J. 2015. *Gypsum efflorescence on clay brick masonry: field survey and literature study*, Constr. Build. Mater. 85: 57 – 64.

Herman, G. T. 2009. *Fundamentals of computerized tomography: image reconstruction from projections*, Springer Science & Business Media.

Kak, A. C. & Slaney, M. 1988. *Principles of computerized tomographic imaging*. IEEE Press.

Pullan, B., Ritchings, R. & Isherwood, I. 1981. *Accuracy and meaning of computed tomography attenuation values*. Technical Aspects of Computed Tomography. Mosby, St. Louis**,** 3904-3917.

Todorović, J., & Janssen, H. 2018. *The impact of salt pore clogging on the hygric properties of bricks*. Construction and Building Materials, 164, 850-863.